PNAS
www.pnas.org

Supplementary Information for

Phosphoproteomics of Arabidopsis Highly ABA-Induced1 identifies AT-Hook Like10 phosphorylation required for stress growth regulation.

Min May Wong[a,b,c], Govinal Badiger Bhaskara [a,1], Tuan-Nan Wen[a], Wen-Dar Lin[a], Thao Thi Nguyen[a,2], Geeng Loo Chong[a,b,c], Paul E. Verslues[a,b,d]

a. Institute of Plant and Microbial Biology, Academia Sinica, Taipei 115, Taiwan
b. Molecular and Biological Agricultural Sciences Program, Taiwan International Graduate Program, National Chung-Hsing University, Taichung 402, Taiwan and Academia Sinica, Taipei 115, Taiwan
c. Graduate Institute of Biotechnology, Biotechnology Center, National Chung-Hsing University, Taichung 402, Taiwan
d. Biotechnology Center, National Chung-Hsing University, Taichung 402, Taiwan

Corresponding author: Paul E. Verslues
Email: paulv@gate.sinica.edu.tw

This PDF file includes:

Supplementary Materials and Methods

References for SI Material and Methods

Figs. S1 to S14

Other supplementary materials for this manuscript include the following:

Datasets S1 to S10

www.pnas.org/cgi/doi/10.1073/pnas.1819971116

SI Appendix: Supplementary Materials and Methods

Quantitative phosphoproteomics using I-Traq labeling

Phosphoproteomic analysis of *hai1-2* was conducted in the same set of experiments as the analysis of *egr1-1egr2-1* (1) with the *hai1-2* and *egr1-egr2-1* samples collected simultaneously along with samples of wild type. Phosphoproteome data of all three genotypes has been deposited to the ProteomeXchange Consortium via the PRIDE partner repository with the data set identifier PXD004869. The wild type phosphoproteome data has also been submitted to PhosPhat (http://phosphat.uni-hohenheim.de/). Microarray analysis of *hai1-2* from the same set of experiments has been previously described (2) and is available on NCBI GEO under accession number GSE35258. In these experiments, seven day old seedlings were transferred to fresh half strength-MS agar plates (control) or PEG infused agar plates (stress, -1.2 MPa) for 96 h before sample collection. Samples were collected from three independent experiments (biological replicates) and the reproducibility of the stress treatment in each biological replicate was confirmed by measuring seedling proline content.

Sample preparation for phosphoproteomics generally followed previous protocols (3) with some modifications as described (1). In brief, after homogenation of samples in liquid nitrogen and trichoroacetic acid (TCA)/acetone solution (10% TCA in acetone containing 0.07% 2-mercaptoethanol), proteins were solubolized using dissolution buffer (9 M Urea, 25 mM Tris-HCl, pH 8.0) containing phosphatase inhibitors (Sigma cocktail 2 and 3). Six mg of total protein for each sample was reduced with 10 mM DTT, alkylated with 25 mM iodoacetamide. Protein digestion was performed by treating with Lys-C endopeptidase followed by trypsin. The tryptic peptides were desalted using a Sep-Pak C18 column and phosphopeptide enrichment performed using a Pierce TiO_2 phosphopeptide enrichment and clean-up kit. Phosphopeptide labeling was done using an AB Sciex iTRAQ 8-plex reagent kit following the manufacturer's instructions. iTRAQ reagents 113/117 were used for wild type control/stress and 115/119 for *hai1-2* control/stress. Samples labeled with individual iTRAQ tags were combined in one tube, desalted using a Pierce graphite spin column, desalted and fractionated by strong cation exchange (PolySULFOETHYL A column, 4.6 x 100 mm, 5 um, 200Å; PolyLC Inc. Columbia, MD) using an elution gradient from 0-50% buffer B (0.35 M KCl in buffer A; buffer B consisted of 7 mM KH2PO4, pH 2.65, 30% acetonitrile). Samples were eluted over 20 min and ten fractions of 0.5 ml each were collected. Each fraction was desalted using a graphite spin column and dried under vacuum.

The SCX fractions were analyzed on a nanoUPLC system (nanoAcquity, Waters, Milford, MA) coupled to an LTQ Orbitrap Velos hybrid mass spectrometer (Thermo Scientific,Bremen, Germany). A C18 capillary column (75 µm x 250 mm, 1.7 µm, BEH130, Waters, Milford, MA) was used to separate peptides with a 90-min linear gradient from 5% to 40% acetonitrile in 0.1% formic acid at a flow rate of 300 nl/min. The operation parameters for the LTQ Orbitrap Velos MS were as previously described (1). Peptide identification, phosphorylation, and quantification were performed using Proteome Discoverer software (v1.3, Thermo Fisher Scientific) with SEQUEST and Mascot (v2.3, Matrix Science) search engines. MS data were searched against TAIR10 protein sequence database with 27,416 sequence entries downloaded from the Arabidopsis Information Resource website (http://www.arabidopsis.org/). The parameters for database searches were set as follows: full trypsin digestion with 2 maximum missed cleavage sites, precursor mass tolerance = 10 ppm, fragment mass tolerance = 0.8 Da (CID) and 50 mmu

(HCD), dynamic modifications: oxidation (M) and phosphorylation (S, T, and Y), static modifications: carbamidomethyl (C), iTRAQ 8-plex (N-terminus and K). The identified peptides were validated using Percolator algorithm which automatically conducted a decoy database search and rescored peptide spectrum matches (PSM) using *q*-values and posterior error probabilities. All the PSMs were filtered with a *q*-value threshold of 0.01 (1% false discovery rate). Phosphopeptides were further validated using phospho*RS* algorithm with thresholds of pRS score ≥ 50 and pRS site probability ≥ 75%. For iTRAQ quantification, the ratios of iTRAQ reporter ion intensities in MS/MS spectra (m/z:113 and 117) from raw datasets were used to calculate the fold changes in phosphorylation between control and treatment. Phosphopeptide abundances were statistically analyzed using a one sample T-test. To estimate the false discovery rates associated with our dataset, q-values were calculated from the characteristics of the p-value distribution using the "*qvalue*" package in the R environment (4). Note however that the q values were used only as in indicator of false discovery rate and were not used to set a specific false discovery threshold to define phosphopeptides of significantly altered abundance. Unadjusted $P \leq 0.05$ and fold change ≥ 1.5 were the criteria used to define phosphopeptides of significantly altered abundance. The PhosPhat database (http://phosphat.uni-hohenheim.de/) (5) was used to find additional experimentally identified AHL10 phosphorylation sites.

Sequence Analysis and Structural Prediction

Enrichment of specific motifs was analyzed using the Motif-X algorithm (6) (http://motif-x.med.harvard.edu/). Sequences were manually centered at the phosphorylated residue and extended 10 amino acids on each side to generate pre-aligned 21 amino acid sequences (Dataset S4). The analysis parameters used were: minimum number of occurrences 5, significance 0.01, Arabidopsis proteome background. Alignment of Clade B AHL amino acid sequences was conducted using T-Coffee (http://www.tcoffee.org/) using the default parameters. Clade B AHL protein sequences were retrieved from Uniprot. BLOcks Substitution Matrix (BLOSUM62) was used to score sequence alignment of proteins and phylogenetic tree generated using average distance algorithm. Multiple sequence alignment of Clade B AHLs was done using Jalview (7). Structural prediction of AHL10 was performed using I-Tasser (8) and visualized in PyMol.

Plant material, growth condition and physiological assays

A T-DNA insertion line in AHL10, *ahl10-1* (SALK_073165C), was obtained from the Arabidopsis Biological Resource Center and the homozygous plants confirmed using primers designed using the Signal web resource; http://signal.salk.edu/. The *hai1-2* mutant (SALK_108282) has been previously described (2). To express *AHL10* under control of its native promoter, a genomic fragment containing the *AHL10* gene body and 2.1 kb of promoter sequence was amplified from Col-0, cloned into pENTR/D-TOPO (Invitrogen), moved to binary vector pGWB540 (9) and transformed into *Agrobacterium tumefaciens* strain GV3101 and then used for floral dip transformation of *ahl10-1*. For cDNA expression, cDNA was prepared from total RNA and the AHL10 cDNA amplified, cloned into pCR8/GW/TOPO (Invitrogen) followed by LR reaction into pEarleyGate104 (10) and transformation into *ahl10-1*. Substitution of Ser-313 (codon AGT) to Ala (codon GCT) or Asp (codon GAT) and Ser-314 (codon AGC) to Ala (codon GCC) or Asp (codon GAC) to generate phosphonull or phosphomimic of AHL10, respectively, was performed by PCR-driven overlap extension (11) using site-directed mutagenic primers and PCR product then transformed into pCR8/GW/TOPO. Plasmids isolated from spectinomycin-resistant colonies were sequenced to confirm the presence of the AHL10

mutation were then transferred by LR reaction to pEarleyGate104. The *hai1-2* mutant was introduced into *AHL10pro*:*AHL10-EYFP/ahl10-1* by crossing. For overexpression of HAI1, the HAI1 cDNA inserted into pEarleyGate 202 (2) was used to transform *AHL10pro*:*AHL10-EYFP/ahl10-1*. All constructs were verified by sequencing. Primers used for genotyping, cloning and site-directed mutagenesis are given in Dataset S10.

Seedling growth and low water potential treatment on PEG-infused agar plates was performed as described previously (1, 12). Growth chamber conditions were 22°C with continuous light at 110-130 μmol photons m^{-2} s^{-1}. For seedling growth assays, five-day-old seedlings were transferred to fresh half-strength MS plates (control, -0.25 MPa) or PEG-infused plates (-0.7 MPa or -1.2 MPa; note that plates were always prepared and infused with PEG for 15 h before use to avoid drying of the media and generate plates of consistent water potential). Root length and fresh weight were measured five days after transfer for control and ten days after transfer for stress treatment. To quantify seedling weight, groups of seedlings were weighed to obtain fresh weight (4-6 seedlings per data point for the unstressed control, 6-7 seedling per data point for the -0.7 MPa treatment and 8-9 seedlings per data point for the -1.2MPa treatment), dried at 65°C and reweighed to obtain dry weight. Wild type seedlings were included on every plate and the growth of each mutant or transgenic line was calculated relative to wild type grown on the same plate to minimize the effect of plate to plate variability in the data. For experiments involving transgenic lines, three independent lines were evaluated for each construct and each line was measured in at least three independent experiments and two or three plates per experiment. Note that in Figure 2, the data from three independent transgenic lines for each construct has been combined. For experiments involving protein or gene expression assays seven-day-old seedlings were transferred to control or stress treatments and samples collected 96 h after transfer.

Controlled soil drying experiments were conducted as previously reported (13). A standard potting mix was combined with 25% Turface (Turface MVP, Profile Products LLC, USA). Four genotypes were planted in sectors (two plants per sector) of 8 cm x 8 cm x 10 cm (LxWxH) plastic pots to ensure that the different genotypes were exposed to the same extent of soil drying. Plants were grown in a short day chamber (8 h light period, 23 C, light intensity of 100-120 μmol m^{-2} sec^{-1}) and Hyponex nutrient solution (1 g $liter^{-1}$) supplied once per week. The position of individual pots within the chamber was rotated every two or three days. On day 19 after planting, pots were watered to saturation, allowed to drain and weighed. Water was withheld for 12 days (leading to 50-60 percent reduction in pot weight), each pot re-watered to 75 percent of the initial pot weight and then allowed to dry another 8-10 day until pot weight again reached 50-60 percent of the starting weight. At the end of the experiment, representative rosettes were photographed and the rest weighed (fresh weight) and then dehydrated in an oven to obtain the dry weight.

Subcellular localization and analysis of protein interaction by ratiometric Bi-molecular Fluorescence Complementation (rBiFC).

Subcellular localization of AHL10 was analyzed in root cells of T_3 homozygous lines. YFP was detected using excitation wavelength of 514 nm at 70% intensity and emission filter of 520-555 nm band pass on a Zeiss LSM 510 META microscope. Ratiometric BiFC (rBiFC) assays were performed using previously described vectors (14). Coding sequences of AHL10 (or

AHL10 phosphonull and phosphomimic) and HAI1 (or HAI2, HAI3) were cloned into pDONR221 P1-P4 and pDONR221 P3-P2 (Invitrogen) respectively (primers used are listed in Dataset S10). These donor vectors were used for LR reaction with the destination vector pBiFCt-2in1-NN. The resulting plasmid was transformed into *Agrobacterium tumefaciens* strain GV3101 and transient expression was performed in 5-day-old seedlings of a line with Dexamethasone (DEX) inducible AvrPto expression (ABRC stock number CS67140) (15). DEX application and Agrobacterium infiltration of seedlings was performed as previously described (16). Seedlings were transferred to fresh control or PEG-infused agar plates (-1.2 MPa) 24 h after infiltration and rBiFC interaction was visualized 48-96 h after transfer. To visualize the rBiFC interaction, YFP was detected on a Zeiss LSM 510 META microscope at excitation wavelength 514 nm (70-80% intensity) and emission filter of 520-555 nm band pass with 450-550 µm pinhole while RFP was detected at excitation wavelength 543 nm (70-80% intensity) and emission filter 560-615 nm band pass with 450-550 µm pinhole. To quantify the rBiFC ratio, fluorescence intensity of YFP and the constitutively expressed RFP reporter was quantified for at least 20 individual cells from 4-5 seedlings combined from at least two independent experiments. For each quantification, a whole cell was selected as a region of interest (ROI) in Image J, the mean intensity of RFP and YFP over the ROI determined (using the analyze/measure function) and the YFP/RFP ratio calculated. Given the emission spectra of YFP and RFP and the filter set used to detect emission, a low level of bleed through from the YFP channel to RFP is unavoidable. In pixels where YFP intensity was very high, this bleed through could be seen in the RFP images. Because this occurred in only a small number of pixels while the rBiFC analysis used RFP intensity over the whole cell, the YFP/RFP ratio used for quantitation of relative interaction intensities was not substantially affected by leakage between the two channels. Also, inspection of pixel by pixel scatter plots of YFP versus RFP intensities showed that leakage from the RFP channel into the YFP channel was minimal and did not affect the visualization of YFP localization. For rBiFC experiments of AHL10 self-interaction, the number of nuclei having two or more visible YFP foci were counted and nuclei not meeting this criteria were considered as having diffuse localization. For the counts of nuclei with AHL10 foci, 95% confidence intervals and significant differences based on Fisher's exact test were determined using GraphPad Quick Calcs (https://www.graphpad.com/quickcalcs/catMenu/).

Additional BiFC analyses were performed in similar manner using pSITE-nEYFP-C1 and pSITE-cEYFP-C1vectors as previously described (1).

Recombinant Protein Expression and Purification

An N-terminal truncation (amino acids 1-103) of HAI1 was used for protein expression. Note that this truncation was similar to that used previously for in vitro expression and activity assays of HAI1 (17) and was necessary to improve HAI1 solubility. $HAI1^{\Delta 1\text{-}103}$ was cloned into pET300NT destination vector (N-terminal HIS tag) and transformed into the *E.coli* strain BL21 (Rosetta DE3). $HAI1^{\Delta 1\text{-}103}$ protein expression was induced by addition of 0.75 mM IPTG when cultures reached an optical density of 0.4. Following overnight incubation at 16 ºC, cells were harvested and resuspended in lysis buffer (50 mM Tris HCl pH 7.5, 250 mM KCl, 0.1% Tween-20, 10% glycerol, 10 mM β-ME, 1× Roche EDTA-free protease inhibitor) and lysed using cell disruptor (Constant Systems). Lysate was filtered and applied to a 5 mL Mini Profinity IMAC cartridge using a BioLogic low pressure chromatography system (Bio-Rad). An imidazole gradient was used to elute the protein in elution buffer **(**50 mM Tris HCl pH 7.5, 20% glycerol,

25 mM $Mg(OAc)_2$, 2 mM $MnCl_2$, 10 mM β-ME, 1X Roche EDTA-free protease inhibitor). Note that no additional salt was added to the eluted protein as salt interferes with phosphatase activity. Phosphatase activity of the recombinant $HAI1^{\Delta 1\text{-}103}$ was tested using a phosphatase assay kit (Biosciences Cat. #786-453).

***In vitro* dephosphorylation of AHL10 and analysis of AHL10 phosphorylation using Phos-Tag polyacrylamide gels.**

To obtain highly phosphorylated AHL10 protein for *in vitro* dephosphorylation assay, seedlings of *AHL10pro*:*AHL10-EYFP/ahl10-1hai1-2*, were collected after 96 h stress treatment, ground in liquid nitrogen and further homogenized in cold extraction buffer (150 mM NaCl, 50 mM Tris HCl pH 7.5, 10% glycerol, 10 mM EDTA, 10 mM DTT, 1mM NaF, 1mM Na_2MoO_4, 1% IGEPAL, 2× Roche EDTA-free protease inhibitor, 2× Roche phosphatase inhibitor). The homogenate was centrifuged and protein content of the supernatant measured using a Pierce 660nm Protein Assay Reagent (Thermo Scientific). For immunoprecipitation of AHL10-YFP, 30 µl of equilibrated GFP-Trap magnetic resin (Chromotek) was added to extract containing 100 µg of total protein and rotated at 4ºC for 3 h. The samples were maintained at 4ºC and the GFP-Trap resin washed four times with washing buffer (100 mM NaCl, 10 mM Tris HCl pH 7.5, 0.5% IGEPAL, 1mM DTT, 1X Roche EDTA-free protease inhibitor, 10% glycerol) followed by an additional wash and resuspension in phosphatase treatment buffer (10 mM Tris HCl pH 7.5, 10% glycerol, 1X Roche EDTA-free protease inhibitor). The GFP-Trap resin and bound protein was then equally divided into separate tubes for mock (no phosphatase) treatment, treatment with 1 µl calf intestinal (CIP, NEB) in 1× cut smart buffer or, treatment with 2.5 or 5.0 µg of purified HAI1 in elution buffer. The tubes containing immunoprecipitate plus CIP or HAI1 (or mock incubation without phosphatase) were incubated in 37ºC for 30 min and the reaction stopped by adding SDS loading buffer and heat inactivation for 10 min at 70°C. For additional analysis of AHL10 phosphorylation, *AHL10pro*:*AHL10-EYFP/ahl10*, *35S:YFP-AHL10* N.M. (not mutated), *35S:YFP-AHL10* S313A and *35S:YFP-AHL10* S314A, were stress treated for 96 h and immunoprecipitated following the protocol described above.

Preparation and use of Mn^{2+}-Phos-Tag polyacrylamide gels and subsequent immunoblot was performed as described previously (18) but with some conditions optimized for AHL10. Phos-Tag gel was prepared using 10 ml of 8% acrylamide and 50 µM Phos-tag for the resolving gel [2.67 mL of 30% acrylamide/bis 37.5:1 (Biorad), 2.5 mL of 1.5 M Tris/HCl pH 8.8, 100 µL of 5 mM Phos-tag™ AAL (Wako), 100 µL of 10 mM $MnCl_2$, 100 µL of 10% SDS, 10 µL TEMED, 25 µL of 10% APS, 4.5 ml of distilled water] and 4 mL of 4.5% acrylamide for the stacking gel (600 µL of 30% acrylamide/bis 37.5:1 (Biorad), 1 mL of 0.5 M Tris/HCl pH 6.8, 40 µL of 10% SDS, 4 µL TEMED, 20 µL of 10% APS and 2.34 mL of distilled water). The gel was run initially at 80 V for 30 min at RT then transferred to 30 V for 16 h at 4°C using 1× running buffer (50mM Tris base pH8.3, 0.1% SDS, 192 mM glycine). The resolving gel was then soaked in 2× 100 mL of transfer buffer (192 mM glycine, 25mM Tris-base pH 8.0, and 10% methanol containing 10 mM EDTA) for 30 min each time and then washed once for 20 min in transfer buffer without EDTA. The gel was then further incubated in 100 mL transfer buffer containing 0.2% (w/v) SDS (two 20-min incubations). Protein was blotted onto PVDF membrane by wet tank procedure at 30 V (at constant voltage) for 16 h at 4°C. Membranes were blocked using 5% nonfat milk and probed with 1:2000 dilution of Roche Anti-GFP (Sigma-Aldrich Cat#. 11814460001) and 1:10000 dilution of anti-mouse HRP secondary antibody.

Normal SDS-PAGE analysis and blotting (with HSC70 as loading control where appropriate) were conducted as previously described (1).

For detection of AHL10 *in vivo* phosphorylation status, seedlings were ground in liquid nitrogen and homogenized in extraction buffer (50 mM Tris HCl pH 7.5, 10% glycerol, 1mM DTT, 1mM NaF, 1% IGEPAL, 1× Roche EDTA-free protease inhibitor, 1× Roche phosphatase inhibitor) and protein content assayed as described above. Twenty-five μg of total protein was heated (70°C, 10 min) in SDS loading buffer and analyzed by Mn^{2+}-Phos-Tag polyacrylamide gel electrophoresis and immunoblotting as described above but with the Phos-Tag gel run for longer time period (20 h).

Immunoblot band intensities were quantified using the Fiji ImageJ package (http://fiji.sc/Fiji). An area of interest around the major band(s) in each lane was designated using the rectangular selection tool. The 'plot lane' option in the gel analyzer menu was used to obtain intensity peaks for each selected band. Peak areas for integration were marked, and peak areas calculated using the wand tool.

RNA sequencing

For RNA sequencing, 7-day-old seedlings of Col-0 wild type and *ahl10-1* were transferred to either fresh control agar plates or to PEG-infused plates (-0.7 MPa) and samples collected 96 h after transfer. Total RNA was extracted using RNeasy Plant Mini Kit (Qiagen) according to the manufacturer's protocol and RNA quality checked by 25S/18S ratio using an Agilent Bioanalyzer 2100 according to manufacturer's procedures. Three independent biological experiments were performed and one sample collected from each experiment and used for library preparation (12 RNAseq libraries prepared). The reproducibility of the stress treatment in each biological replicate was confirmed by measuring seedling fresh weight and dry weight. Library preparation and RNA sequencing was carried out by the High Throughput Genomics Core facility of the Biodiversity Research Center, Academia Sinica following protocols using 3 ug of total RNA for oligo-dT purification of mRNA and library construction by Illumina TruSeq Stranded Total RNA Library Prep Kit. USER digest treatment was performed for adaptor ligation and the final library was amplified by 10 cycles of PCR using KAPA HiFi Mastermix. The sequencing was performed on an Illumina HiSeq 2500 using paired end reads with an average insert size of 250 bp. Base calling and demultiplexing were performed using Illumina CASAVA-Bcl2fastq version 1.8.4. RPKM values were calculated using the RackJ software package (http://rackj.sourceforge.net/) with reads mapped to the TAIR10 genome using Bowtie2 and BLAT with default parameters. Expression comparisons were performed using DESeq2.

Quantitative Reverse Transcriptase-PCR analysis of gene expression

Total RNA was extracted from control or -0.7 MPa stress-treated seedlings using RNeasy Plant Mini Kit (Qiagen). Total RNA (typically 1 μg) was reverse transcribed using SuperScript III (Invitrogen). Real-time quantitative PCR assays were prepared using KAPA SYBR FAST qPCR kit (Kapa Biosystems) and run on an Applied Biosystems QuantStudio 12K QPCR instrument. Gene expression values were calculated using the comparative cycle threshold method following normalization based on *ELF1α* expression. Primers used are given in Dataset S10.

References

1. Bhaskara GB, Nguyen TT, Yang TH, & Verslues PE (2017) Comparative Analysis of Phosphoproteome Remodeling After Short Term Water Stress and ABA Treatments versus Longer Term Water Stress Acclimation. *Frontiers in Plant Science* 8: 523
2. Bhaskara GB, Nguyen TT, & Verslues PE (2012) Unique Drought Resistance Functions of the Highly ABA-Induced Clade A Protein Phosphatase 2Cs. *Plant Physiol* 160(1):379-395.
3. Wu JA, *et al.* (2010) Integrating titania enrichment, iTRAQ labeling, and Orbitrap CID-HCD for global identification and quantitative analysis of phosphopeptides. *Proteomics* 10(11):2224-2234.
4. Storey JD, Bass AJ, Dabney A, Robinson D (2015). *qvalue: Q-value estimation for false discovery rate control*. R package version 2.12.0, http://github.com/jdstorey/qvalue.
5. Durek P, *et al.* (2010) PhosPhAt: the Arabidopsis thaliana phosphorylation site database. An update. *Nucleic Acids Research* 38:D828-D834.
6. Schwartz D & Gygi SP (2005) An iterative statistical approach to the identification of protein phosphorylation motifs from large-scale data sets. *Nature Biotechnology* 23:1391.
7. Waterhouse AM, Procter JB, Martin DMA, Clamp M, & Barton GJ (2009) Jalview Version 2—a multiple sequence alignment editor and analysis workbench. *Bioinformatics* 25(9):1189-1191.
8. Yang JY, *et al.* (2015) The I-TASSER Suite: protein structure and function prediction. *Nature Methods* 12(1):7-8.
9. Nakagawa T, *et al.* (2007) Improved Gateway binary vectors: high-performance vectors for creation of fusion constructs in transgenic analysis of plants. *Bioscience, Biotechnology, and Biochemistry* 71(8):2095-2100.
10. Earley KW, *et al.* (2006) Gateway-compatible vectors for plant functional genomics and proteomics. *Plant J* 45(4):616-629.
11. Heckman KL & Pease LR (2007) Gene splicing and mutagenesis by PCR-driven overlap extension. *Nature Protocols* 2(4):924-932.
12. Verslues PE, Agarwal M, Katiyar-Agarwal S, Zhu J, & Zhu JK (2006) Methods and concepts in quantifying resistance to drought, salt and freezing, abiotic stresses that affect plant water status. *Plant J* 45(4):523-539.
13. Bhaskara GB, Yang T-H, & Verslues PE (2015) Dynamic proline metabolism: importance and regulation in water limited environments. *Frontiers in Plant Science* 6: 484
14. Grefen C & Blatt MR (2012) A 2in1 cloning system enables ratiometric bimolecular fluorescence complementation (rBiFC). *Biotechniques* 53(5):311-314.
15. Tsuda K, *et al.* (2012) An efficient Agrobacterium-mediated transient transformation of Arabidopsis. *Plant J* 69(4):713-719.
16. Kumar MN, Hsieh YF, & Verslues PE (2015) At14a-Like1 participates in membrane-associated mechanisms promoting growth during drought in Arabidopsis thaliana. *Proc Natl Acad Sci USA* 112(33):10545-10550.
17. Antoni R, *et al.* (2012) Selective inhibition of clade A phosphatases type 2C by PYR/PYL/RCAR abscisic acid receptors. *Plant Physiol* 158(2): 970-980.
18. Kinoshita E, Kinoshita-Kikuta E, Takiyama K, & Koike T (2006) Phosphate-binding tag, a new tool to visualize phosphorylated proteins. *Molecular & Cellular Proteomics* 5(4):749-757.

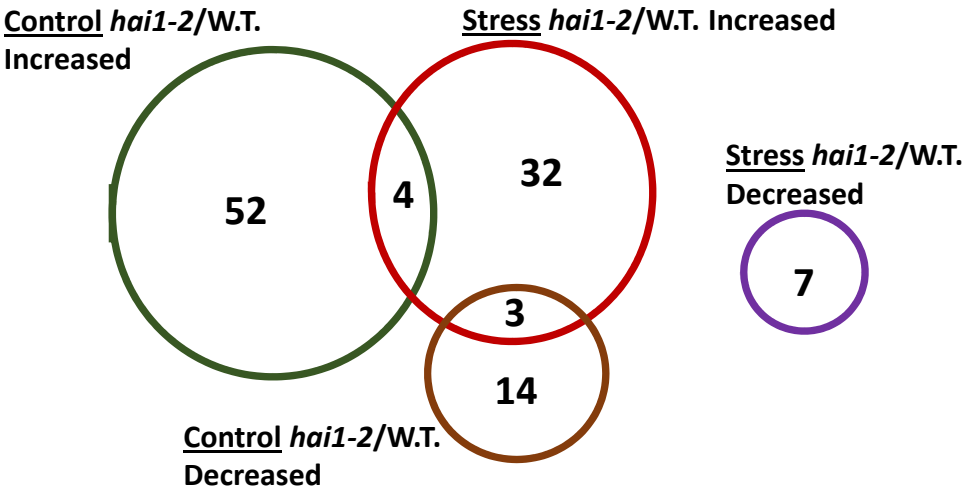

4 Phosphopeptides increased in *hai1-2* control and stress:

AT5G64690.1 neurofilament triplet H protein-like protein

AT1G35580.1 CYTOSOLIC INVERTASE 1 (CINV1);ALKALINE/NEUTRAL INVERTASE G (A/N-InvG), Interacts with PIP5K9.

AT1G17210.1 IAP-LIKE PROTEIN 1 (ILP1)

AT1G51140.1 FLOWERING BHLH 3 (FBH3);ABA-RESPONSIVE KINASE SUBSTRATE 1 (AKS1);ATCFL1 ASSOCIATED PROTEIN 1 (CFLAP1). Basic helix-loop-helix-type transcription factor, DNA-binding capacity is inhibited in response to ABA through phosphorylation-dependent monomerization.

3 Phosphopeptides increased in *hai1-2* stress and decreased in *hai1-2* control:

AT3G55460.1 SC35-LIKE SPLICING FACTOR 30 (At-SCL30);SC35-LIKE SPLICING FACTOR 30 (SCL30). SC35-like splicing factor that is localized to nuclear speckles

AT2G42670.2 PLANT CYSTEINE OXIDASE 4 (PCO4)

AT4G15020.1 hAT transposon superfamily

SI Appendix Figure S1: Overlap between proteins with phosphopeptides of altered abundance in *hai1-2* relative to wild type (W.T.) in the control and stress treatments. Complete lists of phosphopeptides of significantly increased or decreased abundance in *hai1-2* relative to wild type in control and low water potential stress can be found in Datasets S2 and S3.

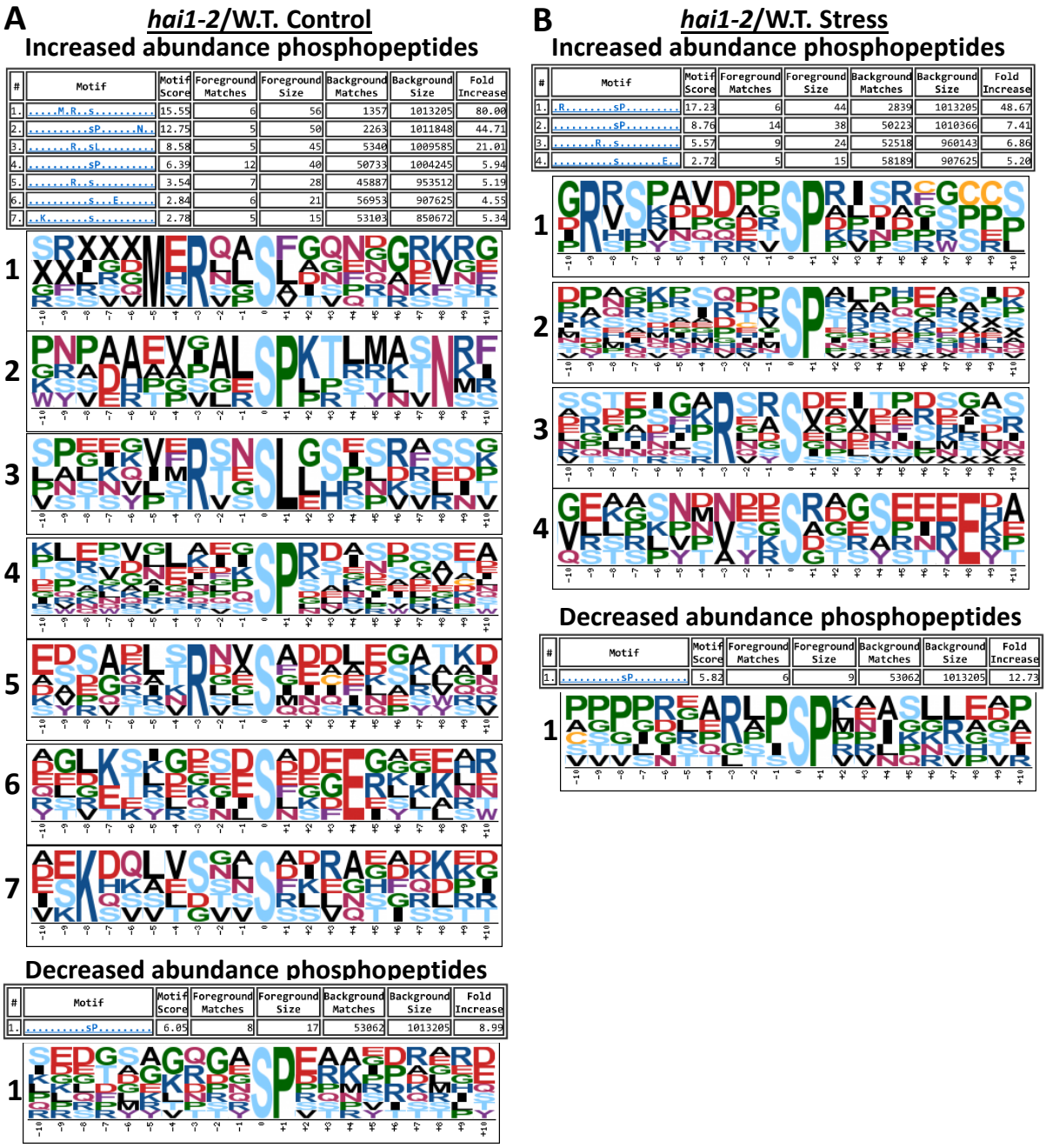

SI Appendix Figure S2: Motif analysis of phosphopeptides of increased or decreased abundance in *hai1-2* relative to wild type. Pre-aligned 21-amino acid sequences (Dataset S4) were submitted to Motif-X to discover overrepresented motifs (analysis parameters: minimum number of occurrences = 5, significance = 0.01, background = Arabidopsis proteome).

A. Motifs found in phosphopeptides of increased or decreased abundance in *hai1-2* in the unstressed control.
B. Motifs found in phosphopeptides of increased or decreased abundance in *hai1-2* under low water potential stress.

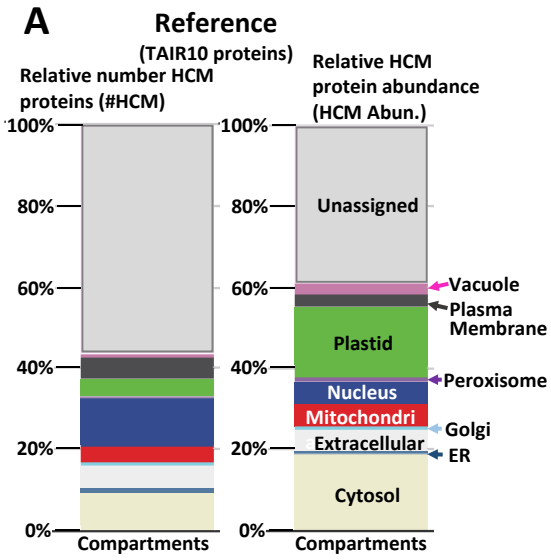

SI Appendix Figure S3: Subcellular localization analysis of putative HAI1 target proteins shows an enrichment of nuclear proteins under stress

Proteins with increased or decreased phosphopeptide abundance in *hai1-2* were submitted to the Multiple Marker Abundance Profiling (MMAP) tool in SUBA (http://suba.live/toolbox-app.html). This tool searches for High Confidence Marker (HCM) proteins and analyzes both their number and relative protein abundance compared to other proteins in the submitted data.

A.Reference data showing localization and relative abundance of all proteins from TAIR10 annotation.

B.Profiles of HCM localization and abundance for proteins with increased or decreased phosphopeptide abundance in *hai1-2* in the unstressed control (Dataset S2).

C.Profiles of HCM localization and abundance for proteins with altered phosphopeptide abundance in *hai1-2* under stress (Dataset S3)

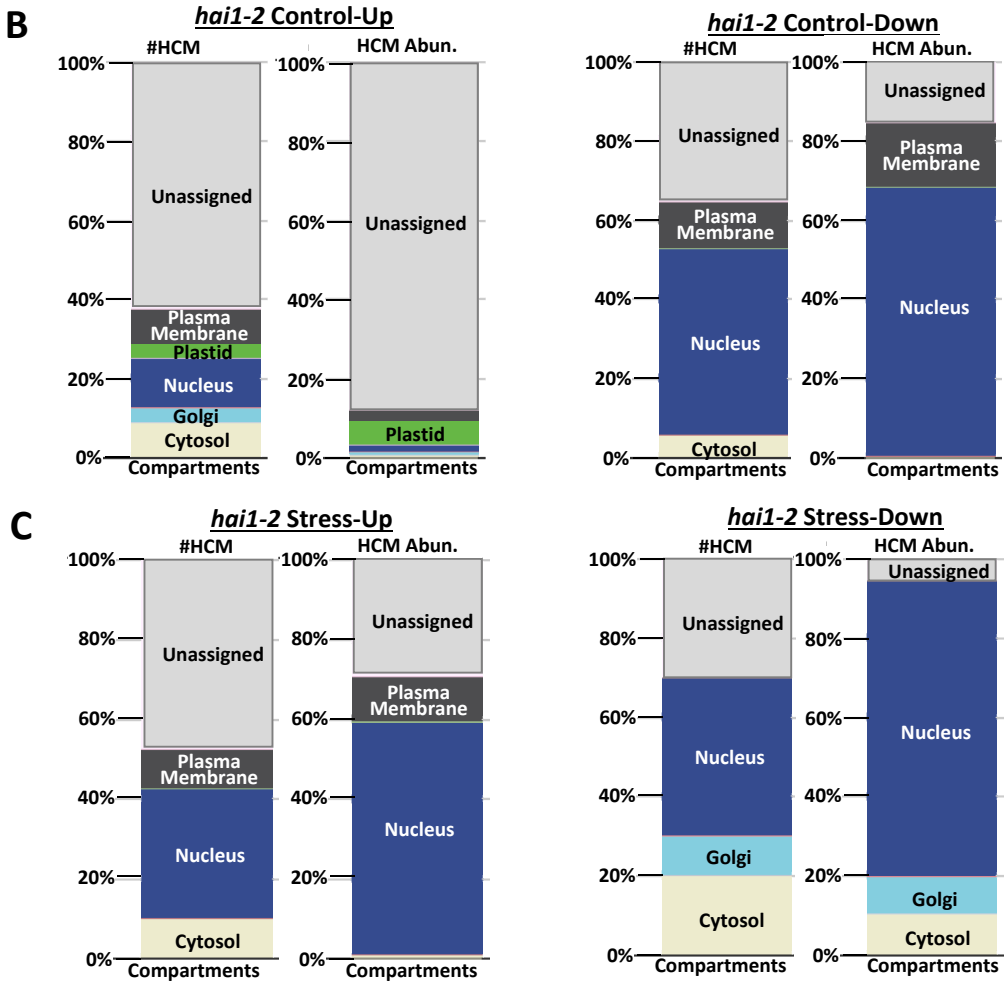

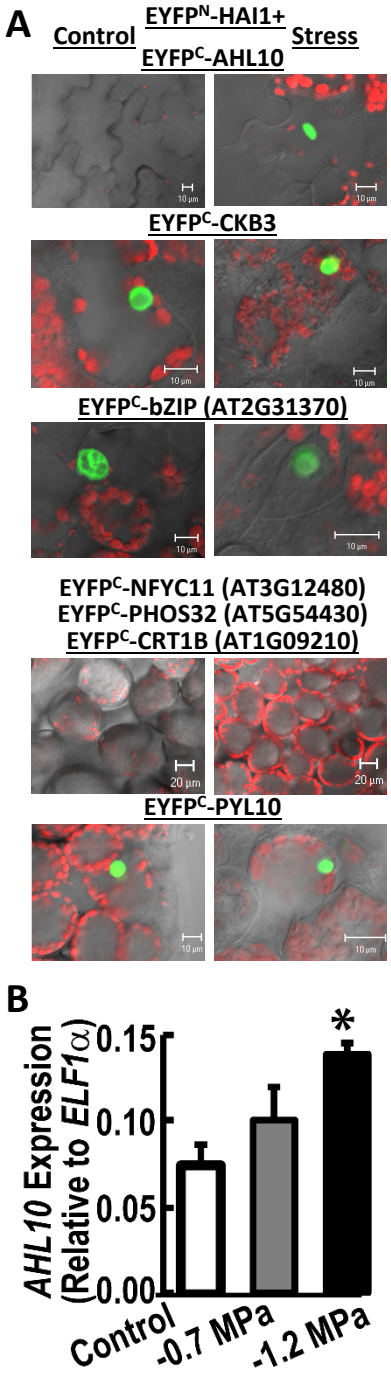

SI Appendix Figure S4: BiFC protein interaction assays for HAI1 and candidate proteins identified by phosphoproteomics.

A. HAI1 and the protein of interest were cloned into the pSITE-nEYFP-C1 and pSITE-cEYFP-C1 vectors, respectively. The constructs were transiently expressed in Arabidopsis seedlings which were then kept under unstressed conditions or exposed to low water potential stress for 72 h. Seven candidate proteins selected based on having increased phosphopeptide abundance in *hai1-2* under either control or stress conditions were tested. Note that for some of these candidates (CRT1B, NFYC11, bZIP) the increase in phosphopeptide abundance was relatively large but not significant in the statistical analysis.

Images shown are leaf mesophyll cells. Green color indicates the BiFC signal while red is chlorophyll autoflourescence. Scale bars show 10 or 20 µm as indicated in each panel. Only one representative image is shown for candidates where interaction could not be observed.

BiFC interaction was seen for HAI1 with AHL10, CKB3 and a bZIP protein. The HAI1-AHL10 interaction was only observed under stress. The interactions were observed in the nucleus consistent with the expected localization of each protein. No interaction was seen for CRT1B, PHOS32 or NFYC11. The known interaction of HAI1 with PYL10 was assayed as a positive control.

B. *AHL10* gene expression in wild type for unstressed control or 96 h after transfer to two different severities of low y_w stress (-0.7 and -1.2 MPa). Data are means ± SE, n = 3. Asterisk (*) indicates significant difference compared to control ($P \leq 0.05$ by T-test).

SI Appendix Figure S5: Spectra of AHL10 phosphopeptides.

A. AHL10 (AT2G33620) S313 phosphorylation Sequence: vAPTQVLMTPsSPQSR, V1-iTRAQ8plex (304.20536 Da), S11-Phospho (79.96633 Da), Charge: +3, Monoisotopic m/z: 695.02277 Da (-0.79 mmu/-1.13 ppm), MH+: 2083.05375 Da, RT: 50.85 min, Identified with: SEQUEST (v1.20); XCorr: 5.16, Probability (FDR q-value): 0.00, Ions matched by search engine: 23/88, Fragment match tolerance used for search: 50 mmu

#1	b+	b2+	b+-P	Seq.	y+	y2+	y+-P	#2
1	404.28106	202.64417		V-iTRAQ8plex				16
2	475.31818	238.16273		A	1679.78232	840.39480	1581.80543	15
3	572.37095	286.68911		P	1608.74520	804.87624	1510.76831	14
4	673.41863	337.21295		T	1511.69243	756.34985	1413.71554	13
5	801.47721	401.24224		Q	1410.64475	705.82601	1312.66786	12
6	900.54563	450.77645		V	1282.58617	641.79672	1184.60928	11
7	1013.62970	507.31849		L	1183.51775	592.26251	1085.54086	10
8	1144.67020	572.83874		M	1070.43368	535.72048	972.45679	9
9	1245.71788	623.36258		T	939.39318	470.20023	841.41629	8
10	1342.77065	671.88896		P	838.34550	419.67639	740.36861	7
11	1509.76901	755.38814	1411.79211	S-Phospho	741.29273	371.15000	643.31584	6
12	1596.80104	798.90416	1498.82414	S	574.29437	287.65082		5
13	1693.85381	847.43054	1595.87691	P	487.26234	244.13481		4
14	1821.91239	911.45983	1723.93549	Q	390.20957	195.60842		3
15	1908.94442	954.97585	1810.96752	S	262.15099	131.57913		2
16				R	175.11896	88.06312		1

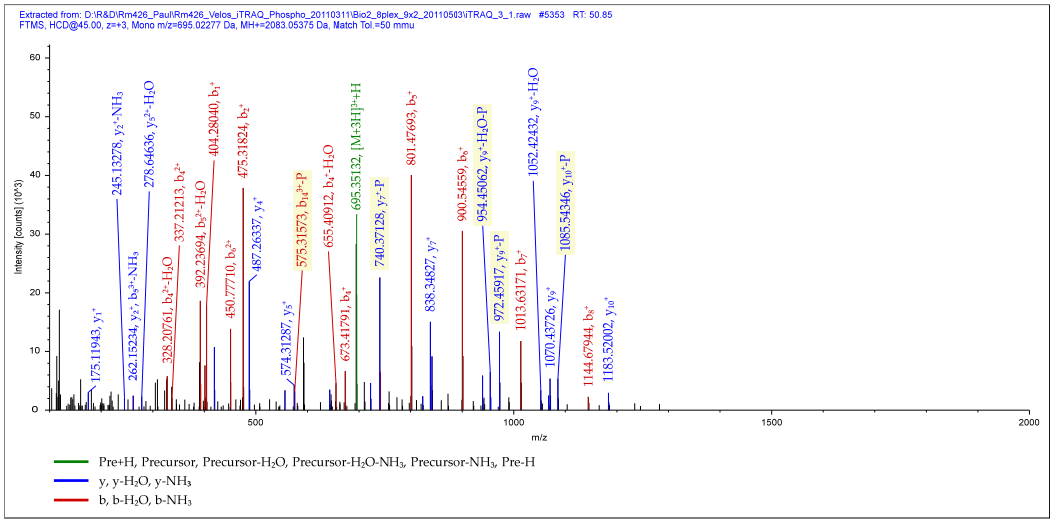

B. AHL10 (AT2G33620) S314 phosphorylation Sequence: vAPTQVLmTPSsPQSR, V1-iTRAQ8plex (304.20536 Da), M8-Oxidation (15.99492 Da), S12-Phospho (79.96633 Da), Charge: +3, Monoisotopic m/z: 700.35394 Da (-1.25 mmu/-1.78 ppm), MH+: 2099.04728 Da, RT: 42.91 min, Identified with: SEQUEST (v1.20); XCorr:5.54, Probability (FDR q-value): 0.00, Ions matched by search engine: 26/88, Fragment match tolerance used for search: 50 mmu

#1	b+	b2+	b+-P	Seq.	y+	y2+	y+-P	#2
1	404.28106	202.64417		V-iTRAQ8plex				16
2	475.31818	238.16273		A	1695.77724	848.39226	1597.80034	15
3	572.37095	286.68911		P	1624.74012	812.87370	1526.76322	14
4	673.41863	337.21295		T	1527.68735	764.34731	1429.71045	13
5	801.47721	401.24224		Q	1426.63967	713.82347	1328.66277	12
6	900.54563	450.77645		V	1298.58109	649.79418	1200.60419	11
7	1013.62970	507.31849		L	1199.51267	600.25997	1101.53577	10
8	1160.66511	580.83619		M-Oxidation	1086.42860	543.71794	988.45170	9
9	1261.71279	631.36003		T	939.39318	470.20023	841.41629	8
10	1358.76556	679.88642		P	838.34550	419.67639	740.36861	7
11	1445.79759	723.40243		S	741.29273	371.15000	643.31584	6
12	1612.79595	806.90161	1514.81906	S-Phospho	654.26070	327.63399	556.28381	5
13	1709.84872	855.42800	1611.87183	P	487.26234	244.13481		4
14	1837.90730	919.45729	1739.93041	Q	390.20957	195.60842		3
15	1924.93933	962.97330	1826.96244	S	262.15099	131.57913		2
16				R	175.11896	88.06312		1

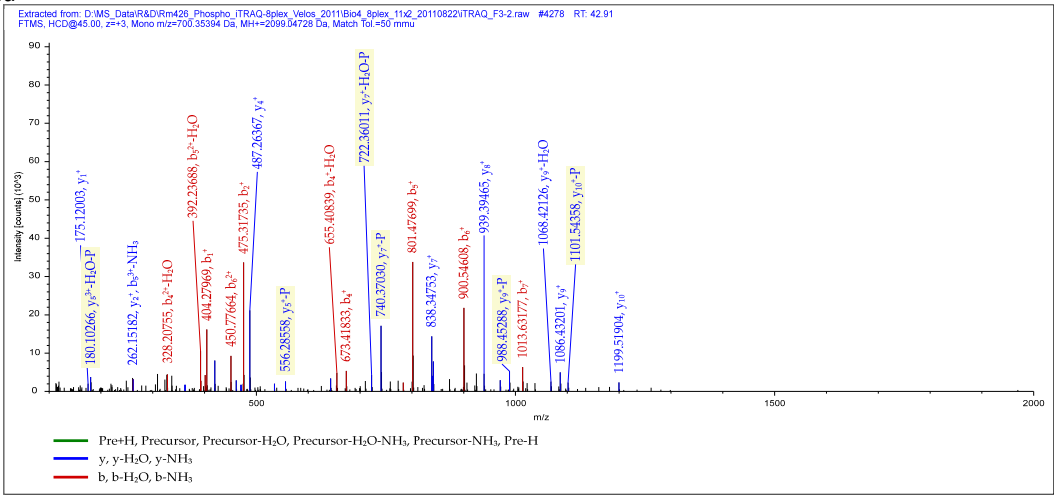

SI Appendix Figure S6: AHL13 phosphopeptide spectra.

A. Sequence: aQNTPEPASAPANmLSFGGVGGPGsPR, A1-iTRAQ8plex (304.20536 Da), M14-Oxidation (15.99492 Da), S25-Phospho (79.96633 Da), **Charge: +4**, Monoisotopic m/z: 742.60388 Da (-0.94 mmu/-1.27 ppm), MH+: 2967.39370 Da, RT: 49.06 min, Identified with: SEQUEST (v1.20); XCorr:8.23, Probability (FDR q-value): 0.00, Ions matched by search engine: 38/231, Fragment match tolerance used for search: 50 mmu

#1	b+	b2+	b+-P	b2+-P	Seq.	y+	y2+	y+-P	y2+-P	#2
1	376.24976	188.62852			A-iTRAQ8plex					27
2	504.30834	252.65781			Q	2592.15499	1296.58113	2494.17809	1247.59268	26
3	618.35127	309.67927			N	2464.09641	1232.55184	2366.11951	1183.56339	25
4	719.39895	360.20311			T	2350.05348	1175.53038	2252.07658	1126.54193	24
5	816.45172	408.72950			P	2249.00580	1125.00654	2151.02890	1076.01809	23
6	945.49432	473.25080			E	2151.95303	1076.48015	2053.97613	1027.49170	22
7	1042.54709	521.77718			P	2022.91043	1011.95885	1924.93353	962.97040	21
8	1113.58421	557.29574			A	1925.85766	963.43247	1827.88076	914.44402	20
9	1200.61624	600.81176			S	1854.82054	927.91391	1756.84364	878.92546	19
10	1271.65336	636.33032			A	1767.78851	884.39789	1669.81161	835.40944	18
11	1368.70613	684.85670			P	1696.75139	848.87933	1598.77449	799.89088	17
12	1439.74325	720.37526			A	1599.69862	800.35295	1501.72172	751.36450	16
13	1553.78618	777.39673			N	1528.66150	764.83439	1430.68460	715.84594	15
14	1700.82159	850.91443			M-Oxidation	1414.61857	707.81292	1316.64167	658.82447	14
15	1813.90566	907.45647			L	1267.58315	634.29521	1169.60626	585.30677	13
16	1900.93769	950.97248			S	1154.49908	577.75318	1056.52219	528.76473	12
17	2048.00611	1024.50669			F	1067.46705	534.23716	969.49016	485.24872	11
18	2105.02758	1053.01743			G	920.39863	460.70295	822.42174	411.71451	10
19	2162.04905	1081.52816			G	863.37716	432.19222	765.40027	383.20377	9
20	2261.11747	1131.06237			V	806.35569	403.68148	708.37880	354.69304	8
21	2318.13894	1159.57311			G	707.28727	354.14727	609.31038	305.15883	7
22	2375.16041	1188.08384			G	650.26580	325.63654	552.28891	276.64809	6
23	2472.21318	1236.61023			P	593.24433	297.12580	495.26744	248.13736	5
24	2529.23465	1265.12096			G	496.19156	248.59942	398.21467	199.61097	4
25	2696.23301	1348.62014	2598.25612	1299.63170	S-Phospho	439.17009	220.08868	341.19320	171.10024	3
26	2793.28578	1397.14653	2695.30889	1348.15808	P	272.17173	136.58950			2
27					R	175.11896	88.06312			1

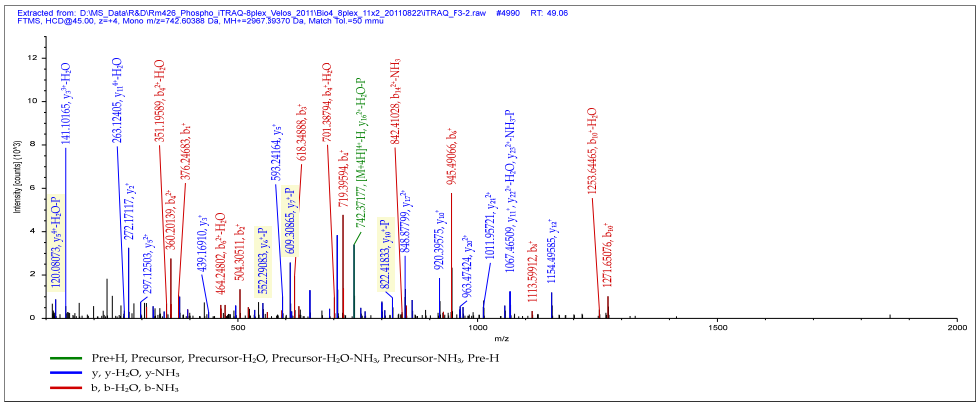

B. Sequence: aQNTPEPASAPANmLSFGGVGGPGsPR, A1-iTRAQ8plex (304.20536 Da), M14-Oxidation (15.99492 Da), S25-Phospho (79.96633 Da), **Charge: +3**, Monoisotopic m/z: 989.80469 Da (+0.68 mmu/+0.69 ppm), MH+: 2967.39951 Da, RT: 48.72 min, Identified with: SEQUEST (v1.20); XCorr:7.00, Probability (FDR q-value): 0.00, Ions matched by search engine: 35/154, Fragment match tolerance used for search: 50 mmu

#1	b+	b2+	b+-P	b2+-P	Seq.	y+	y2+	y+-P	y2+-P	#2
1	376.24976	188.62852			A-iTRAQ8plex					27
2	504.30834	252.65781			Q	2592.15499	1296.58113	2494.17809	1247.59268	26
3	618.35127	309.67927			N	2464.09641	1232.55184	2366.11951	1183.56339	25
4	719.39895	360.20311			T	2350.05348	1175.53038	2252.07658	1126.54193	24
5	816.45172	408.72950			P	2249.00580	1125.00654	2151.02890	1076.01809	23
6	945.49432	473.25080			E	2151.95303	1076.48015	2053.97613	1027.49170	22
7	1042.54709	521.77718			P	2022.91043	1011.95885	1924.93353	962.97040	21
8	1113.58421	557.29574			A	1925.85766	963.43247	1827.88076	914.44402	20
9	1200.61624	600.81176			S	1854.82054	927.91391	1756.84364	878.92546	19
10	1271.65336	636.33032			A	1767.78851	884.39789	1669.81161	835.40944	18
11	1368.70613	684.85670			P	1696.75139	848.87933	1598.77449	799.89088	17
12	1439.74325	720.37526			A	1599.69862	800.35295	1501.72172	751.36450	16
13	1553.78618	777.39673			N	1528.66150	764.83439	1430.68460	715.84594	15
14	1700.82159	850.91443			M-Oxidation	1414.61857	707.81292	1316.64167	658.82447	14
15	1813.90566	907.45647			L	1267.58315	634.29521	1169.60626	585.30677	13
16	1900.93769	950.97248			S	1154.49908	577.75318	1056.52219	528.76473	12
17	2048.00611	1024.50669			F	1067.46705	534.23716	969.49016	485.24872	11
18	2105.02758	1053.01743			G	920.39863	460.70295	822.42174	411.71451	10
19	2162.04905	1081.52816			G	863.37716	432.19222	765.40027	383.20377	9
20	2261.11747	1131.06237			V	806.35569	403.68148	708.37880	354.69304	8
21	2318.13894	1159.57311			G	707.28727	354.14727	609.31038	305.15883	7
22	2375.16041	1188.08384			G	650.26580	325.63654	552.28891	276.64809	6
23	2472.21318	1236.61023			P	593.24433	297.12580	495.26744	248.13736	5
24	2529.23465	1265.12096			G	496.19156	248.59942	398.21467	199.61097	4
25	2696.23301	1348.62014	2598.25612	1299.63170	S-Phospho	439.17009	220.08868	341.19320	171.10024	3
26	2793.28578	1397.14653	2695.30889	1348.15808	P	272.17173	136.58950			2
27					R	175.11896	88.06312			1

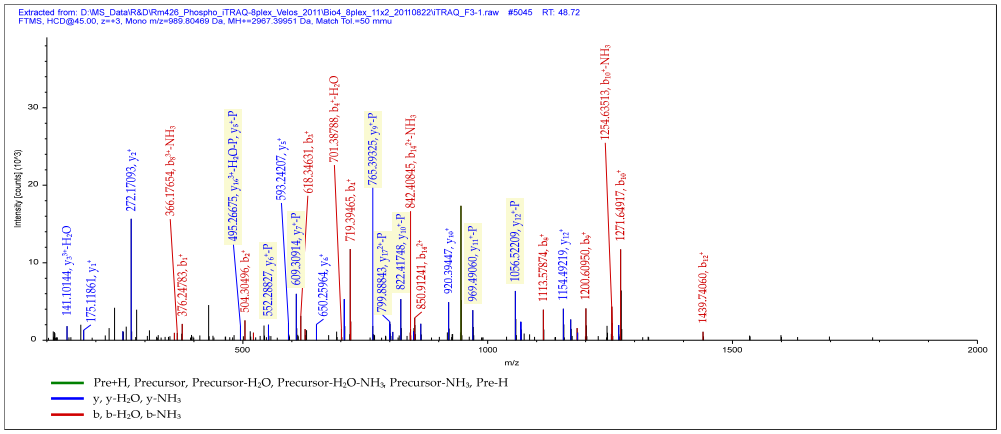

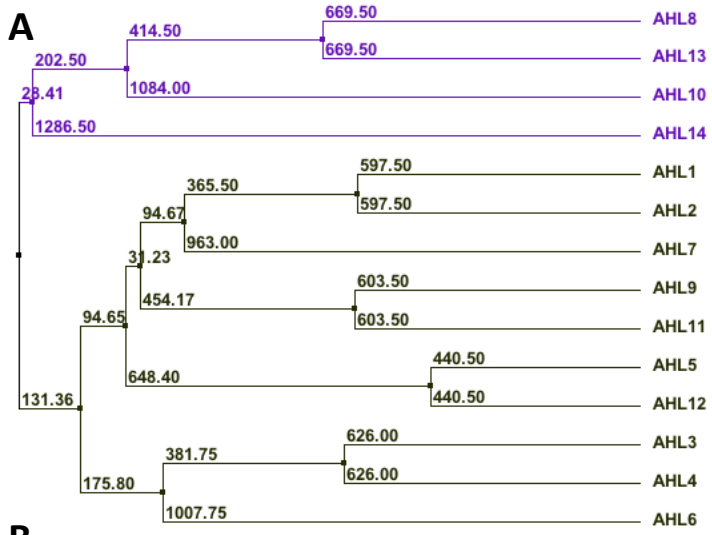

SI Appendix Figure S7: Alignment of Clade B AHLs and location of AHL10/13 phosphorylation site.

A. Phylogenetic tree of Clade B AHLs
B. Alignment of Clade B AHL protein sequences. The red box marks the AHL10 S313/S314 phosphorylation sites. Positions of the two AT-hook domains and PPC/DUF296 domain are also marked.

B

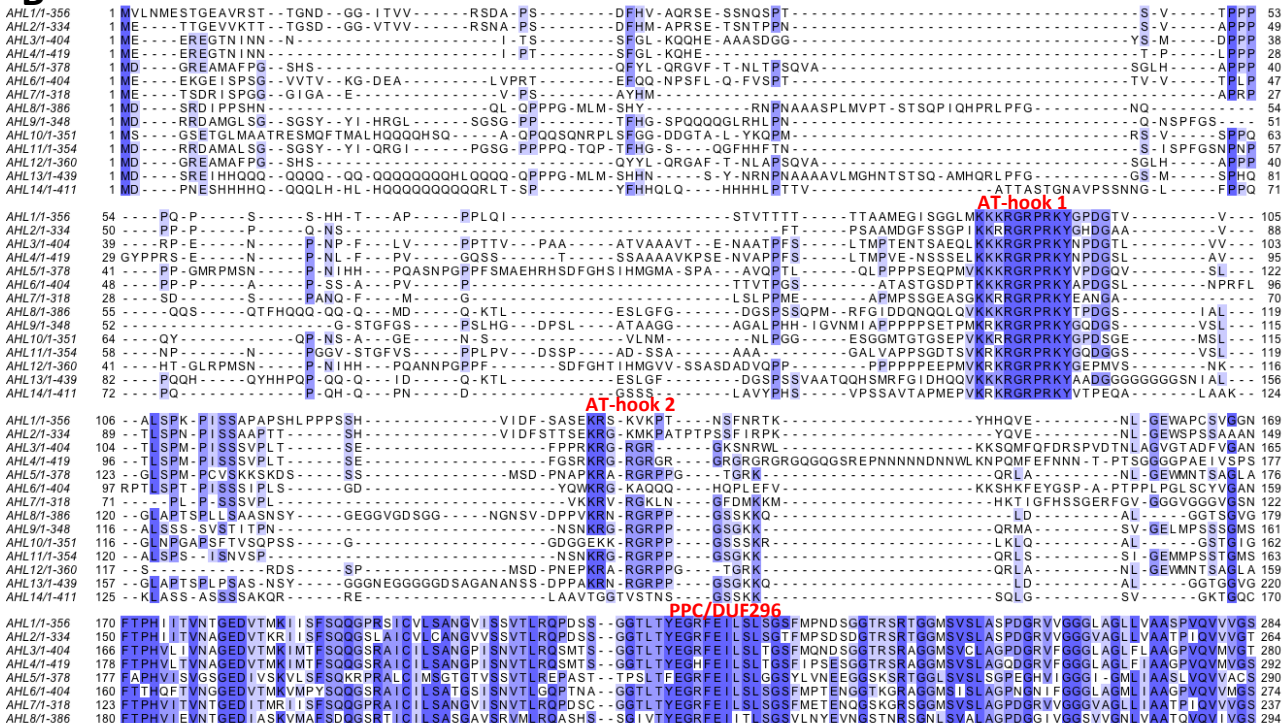

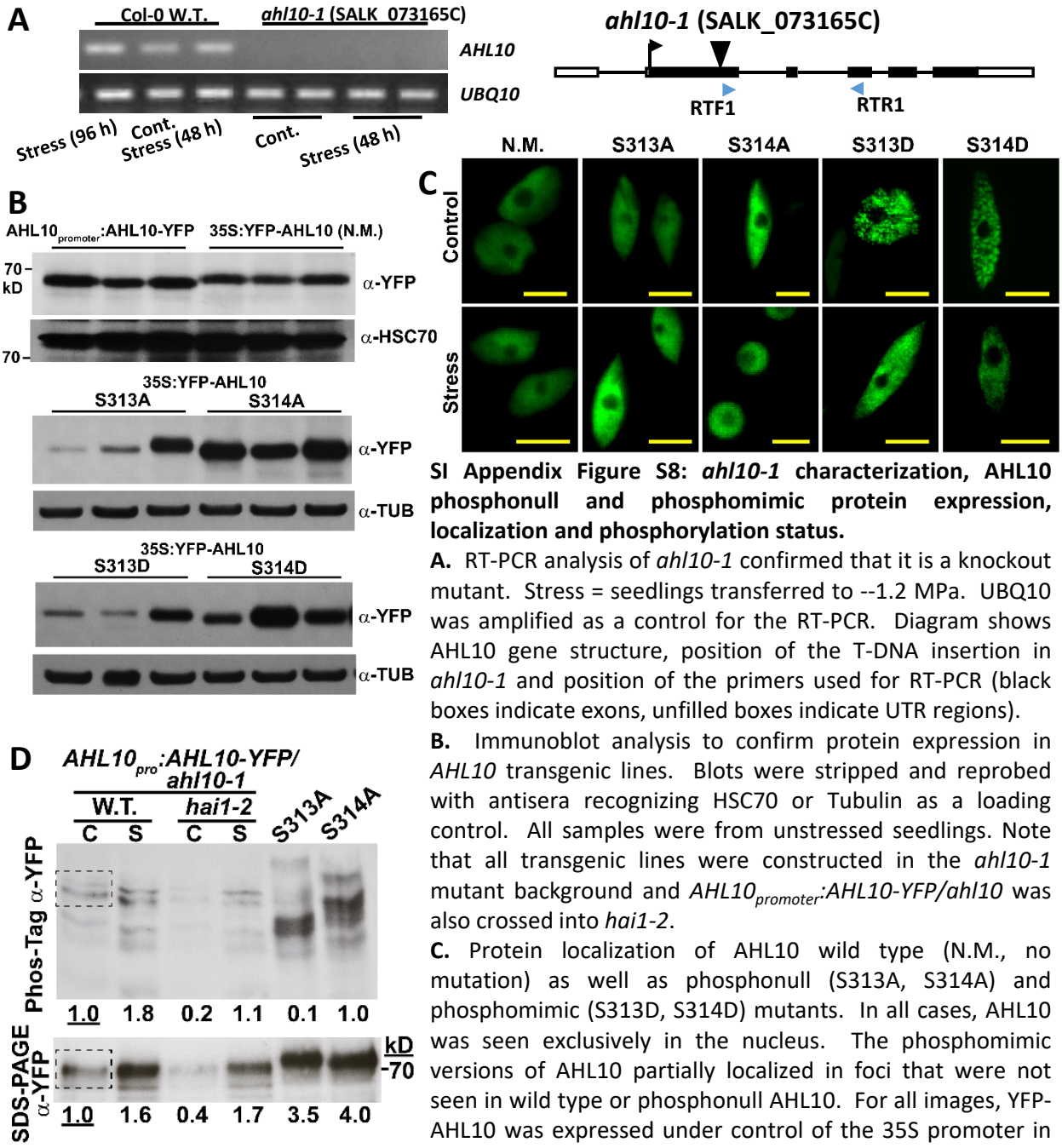

SI Appendix Figure S8: *ahl10-1* characterization, AHL10 phosphonull and phosphomimic protein expression, localization and phosphorylation status.

A. RT-PCR analysis of *ahl10-1* confirmed that it is a knockout mutant. Stress = seedlings transferred to --1.2 MPa. UBQ10 was amplified as a control for the RT-PCR. Diagram shows AHL10 gene structure, position of the T-DNA insertion in *ahl10-1* and position of the primers used for RT-PCR (black boxes indicate exons, unfilled boxes indicate UTR regions).

B. Immunoblot analysis to confirm protein expression in *AHL10* transgenic lines. Blots were stripped and reprobed with antisera recognizing HSC70 or Tubulin as a loading control. All samples were from unstressed seedlings. Note that all transgenic lines were constructed in the *ahl10-1* mutant background and *AHL10$_{promoter}$:AHL10-YFP/ahl10* was also crossed into *hai1-2*.

C. Protein localization of AHL10 wild type (N.M., no mutation) as well as phosphonull (S313A, S314A) and phosphomimic (S313D, S314D) mutants. In all cases, AHL10 was seen exclusively in the nucleus. The phosphomimic versions of AHL10 partially localized in foci that were not seen in wild type or phosphonull AHL10. For all images, YFP-AHL10 was expressed under control of the 35S promoter in the *ahl10-1* background (*35S:YFP-AHL10/ahl10-1*) .

D. Immunoprecipitation of AHL10 from *AHL10$_{promoter}$:AHL10-YFP/ahl10-1 (*in W.T. or *hai1-2* background*)* plants from the unstressed control or -0.7 MPa stress treatment. 100 μg of total protein was used for each immunoprecipiation. For comparision, AHL10 S3134 and S314A were immunoprecipitated from seedlings exposed to -0.7 MPa. The experiment was repeated with consistent results. The dashed box in the wild type control lane indicates the region selected from each lane for quantification of band intensities. Relative band intensities are indicated by the numbers below each lane.

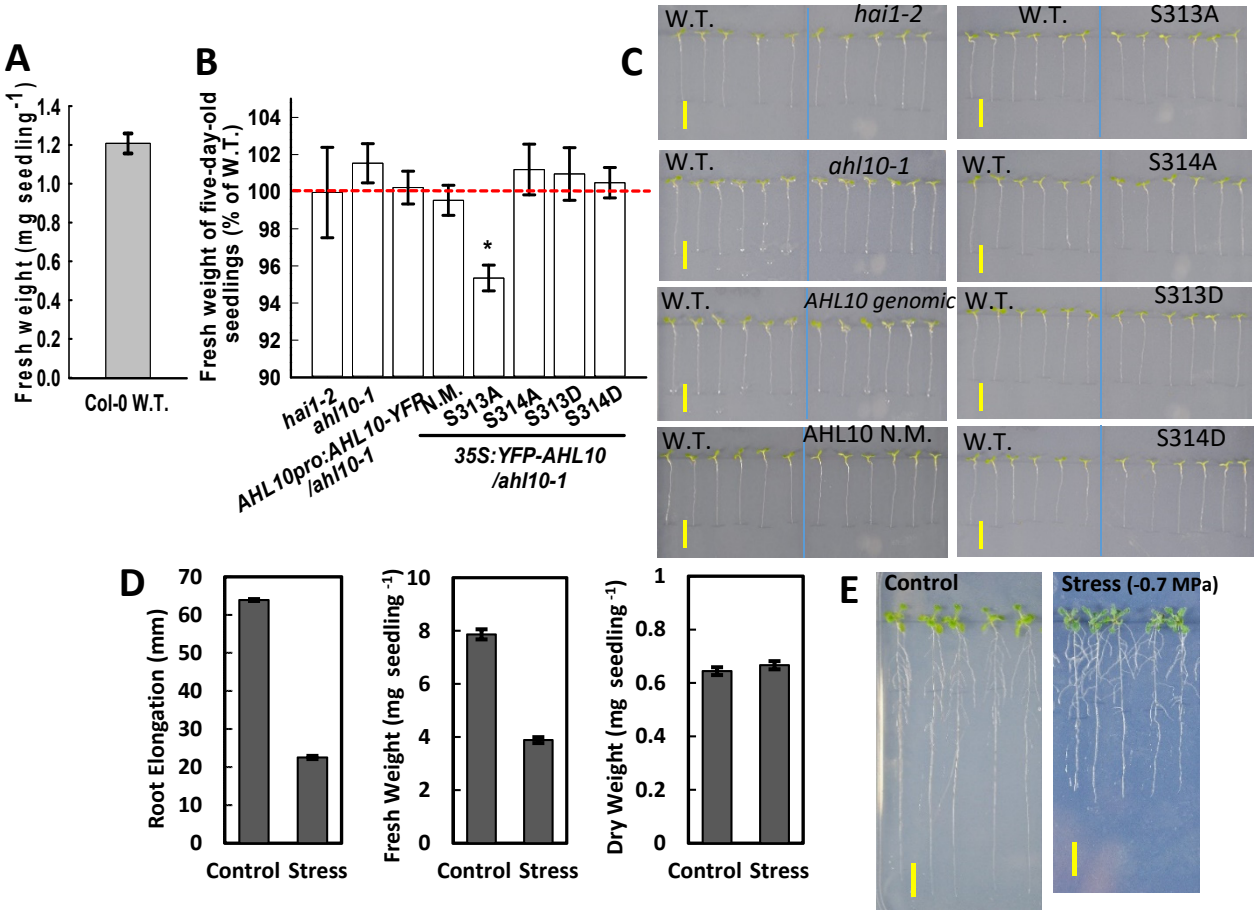

SI Appendix Figure S9: Wild type growth data used to normalize the PEG-agar plate assay data for mutant and transgenic lines shown in Figure 2, fresh weight of 5-day-old seedlings before transfer to stress.

A. Fresh weight of 5-day-old Col-0 W.T. seedlings at the time of transfer to stress or control treatments for PEG-plate growth assays. (mean ± SE, n = 280)

B. Fresh weights of five-day-old seedlings at the time of transfer to stress and control treatments in the PEG-plate growth assays. Data are relative to the Col-0 wild type (W.T.) grown on the same plates as the genotype assayed (mean ± SE, n = 35 to 40, combined from three independent experiments). Asterisk (*) indicates significant difference compared with the wild type by one-sided T-test ($P \leq 0.05$). Dashed red line indicates the wild type level (100%).

C. Representative five-day-old seedlings on a half-strength MS agar plates. "AHL10 genomic" is *AHL10*$_{promoter}$*:AHL10-YFP/ahl10-1.* Other transgenic lines are non-mutated (N.M.), phosphonull (S313A, S314A) and phosphomimic (S313D, S314D) AHL10 expressed under control of 35S promoter in the *ahl10-1* mutant background (*35S:YFP-AHL10/ahl10-1*). Scale bars indicate 1cm.

D. Wild type (Col-0) root elongation, seedling fresh weight and dry weight. Five-day-old seedlings were transferred to either fresh control media (-0.25 MPa) or moderate severity low water potential stress (-0.7 MPa). Root elongation was measured over the following 5 days for control and 10 days for stress. Fresh weight and dry weigh were measured for groups of 5-6 seedlings collected at the end of the experiment. Data are combined from six representative experiments (mean ± S.E.; n = 435-650 for root elongation and 125-190 for fresh and dry weight). Comparison of this data to the fresh weight at the time of transfer (A) shows that the seedlings continued to grow and increase in fresh weight at -0.7 MPa but at a reduced rate compared to control. Seedlings allowed to grow for 10 days after transfer to -0.7 MPa were able to accumulate a similar total dry weight as unstressed seedlings harvested at 5 days after transfer.

E. Representative pictures of wild type seedlings under control or stress conditions. Photos were taken at the end of experiment (5 days after transfer for control, 10 days after transfer for stress). Black lines along the root indicate the position of the primary root apex at the time of transfer. Scale bars indicate 1 cm.

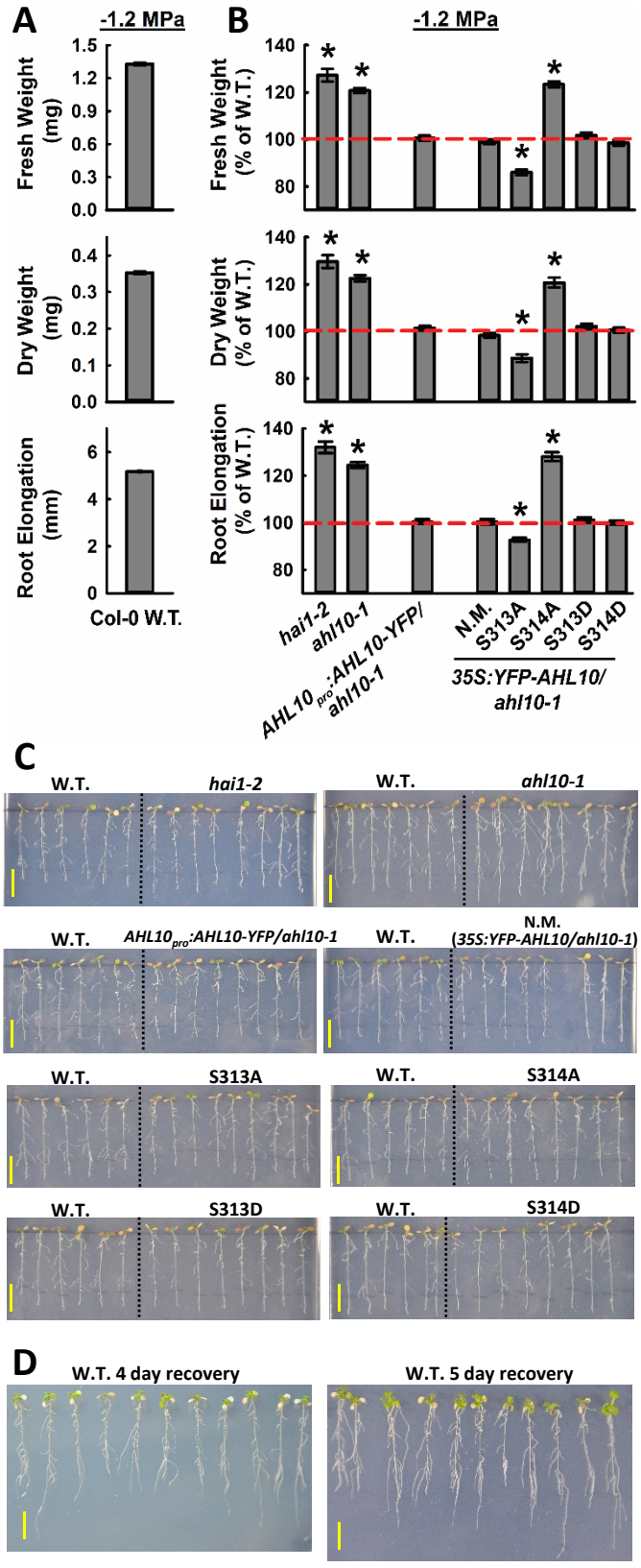

SI Appendix Figure S10: Growth of AHL10 mutant and transgenic lines after transfer to -1.2 MPa PEG-agar plates.

A. Fresh weight, dry weight and root elongation data of Col-0 W.T. used to normalize the data in B. Five-day-old seedlings were transferred to -1.2 MPa agar plates and growth parameters measured 10 days later. Data are mean ± SE, n = 139 for fresh weight and dry weight, n = 835 for root elongation, combined from two independent experiments.

B. Relative fresh weight, dry weight and root elongation of AHL10 and HAI1 mutant and transgenic lines 10 days after transfer of 5-day-old seedlings to -1.2 MPa agar plates. Data are presented relative to wild type seedlings assayed in the same PEG-agar plates (dashed red line indicates the wild type level, 100%). Data are mean ± SE, n = 6-10 combined from two independent experiments. Asterisk (*) indicates significant difference compared with the wild type by one-sample T-test ($P \leq 0.05$). Dashed red line indicates the wild type level (100%). N.M. = Non mutated (wild type) AHL10.

C. Representative images of Col-0 wild type (W.T.) and mutant/transgenic seedlings. Five day-old seedlings were transferred to -1.2 MPa agar plates for 10 days before photographs were taken. Images are from the same experiments shown in A and B. Scale bars indicate 1 cm. Black lines behind the roots indicated the position of the root apices at the time of transfer.

D. Representative images of seedlings subjected to -1.2 MPa stress for 10 days as described above and then transferred back to unstressed control media to determine the ability of the seedlings to recover and resume growth. Several independent experiments were performed and 100% of seedlings were alive and recovered in all cases. Photographs were taken 4 or 5 days after transfer back to the control media, as indicated. Scale bars indicate 1 cm.

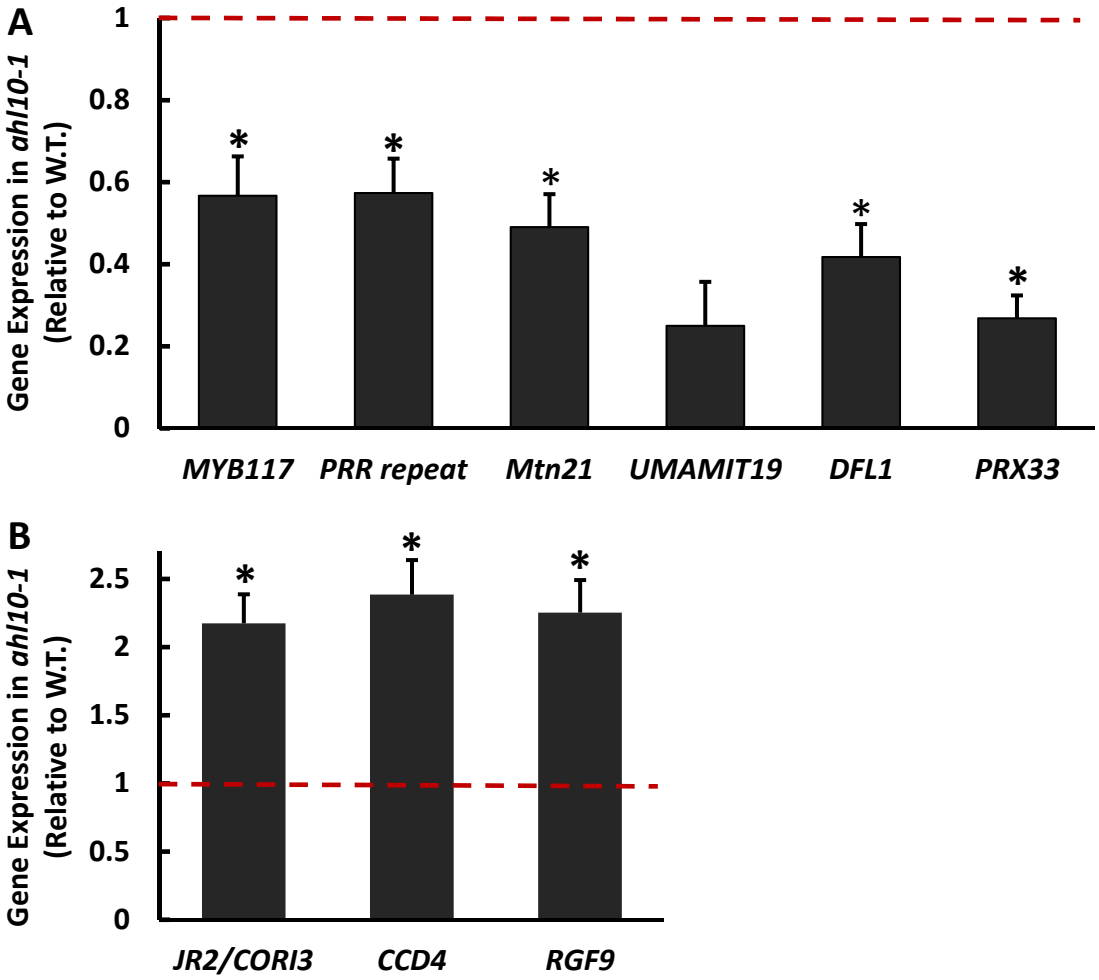

SI Appendix Figure S11: Validation of additional gene expression changes in *ahl10-1* at low water potential.

A. QPCR assay of genes found to be down-regulated in *ahl10-1* during stress by RNAseq (Dataset S9). Seedlings were transferred to -0.7 MPa for 96 h and gene expression assayed. Data are means ± S.E., n =3 from 3 independent experiments. Expression data are relative to wild type assayed in the same experiment. Red dashed line indicates the wild type expression level (set to 1). Asterisks (*) indicate significant difference relative to wild type (by one-sided T-test, $P \leq 0.05$).

B. QPCR assay of genes found to be up-regulated in *ahl10-1* during stress by RNAseq (Dataset S9). Data format is the same as in A.

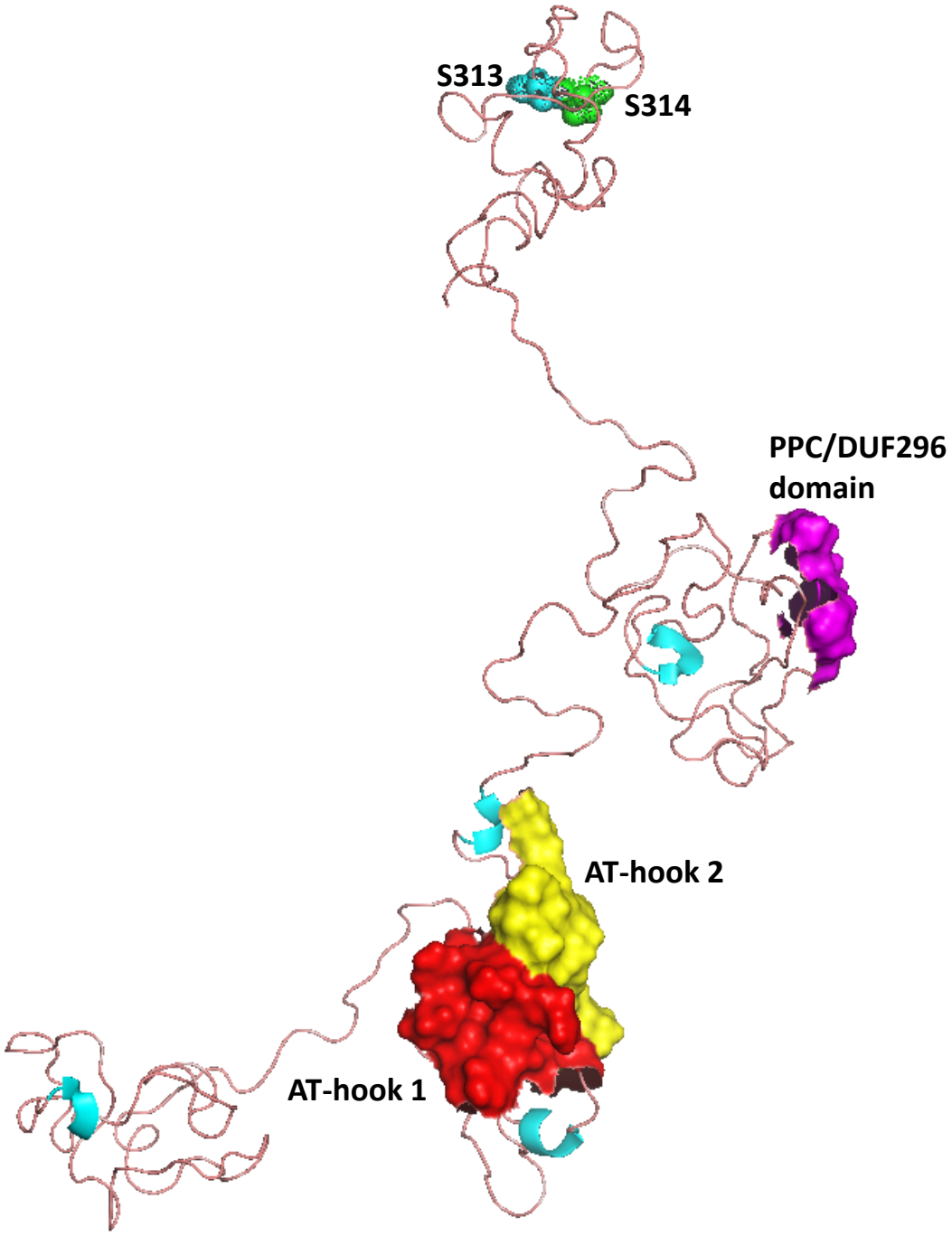

SI Appendix Figure S12: Predicted AHL10 structure and location of the S313 and S314 phosphorylation sites.

AHL10 predicted structure indicates that in the tertiary structure of AHL10 the phosphorylation sites at S313 and S314 in the C-terminal loop region are not adjacent to the PPC/DUF296 domain involved in AHL multimerization nor the AT-hook domains involved in DNA binding.

AHL10 structure was predicted by I-Tasser and visualized by PyMOL. Color coding: Helices: Cyan, Loops: Wheat (pink), AT-hook1: Red surface, AT-hook2: Yellow surface PPC/DUF296 domain: magenta surface.

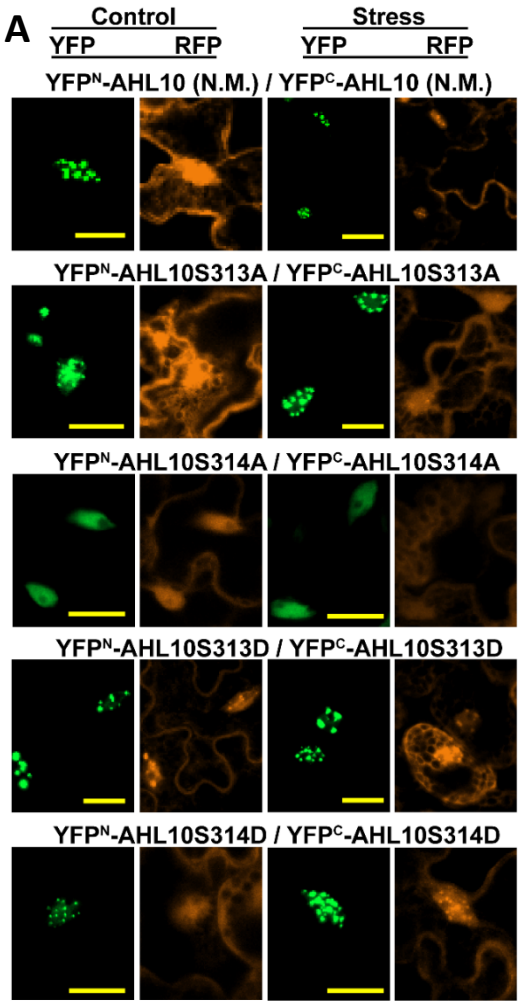

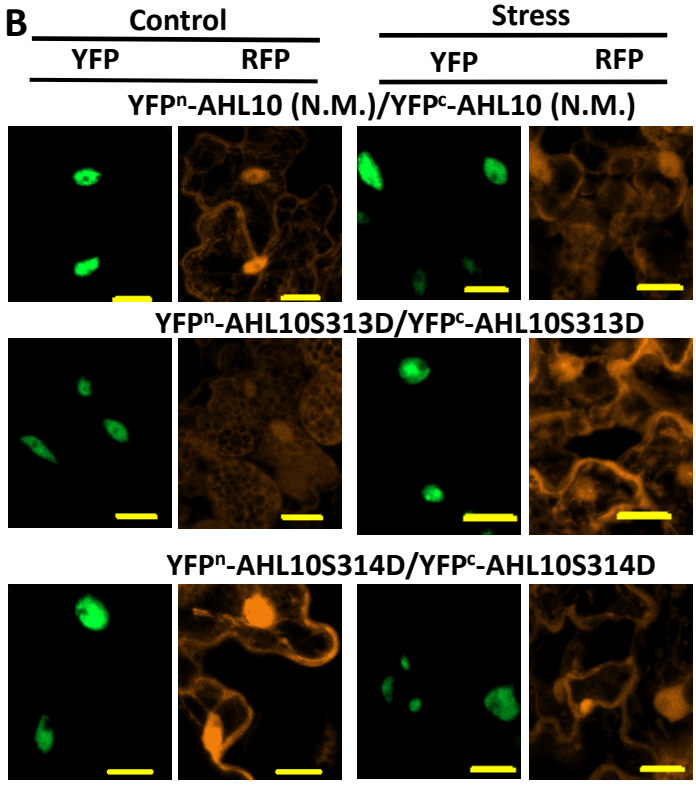

SI Appendix Figure S13: Representative images of AHL10 self interaction in rBiFC assays.

A. Representative images of AHL10 self-interactions (YFP) and constitutively expressed RFP used to normalize the interaction intensity. These images show representative examples of nuclei with AHL10 foci (except for S314A where nuclear foci were never observed). Scale bars indicate 20 μm.

B. Representative images of nuclei without foci for non-mutated AHL10 (N.M.) as well as the two phosphomimic AHL10 constructs. Scale bars indicate 20 μm.

Quantification of the proportion of nuclei with and without foci is shown in Fig. 4C.

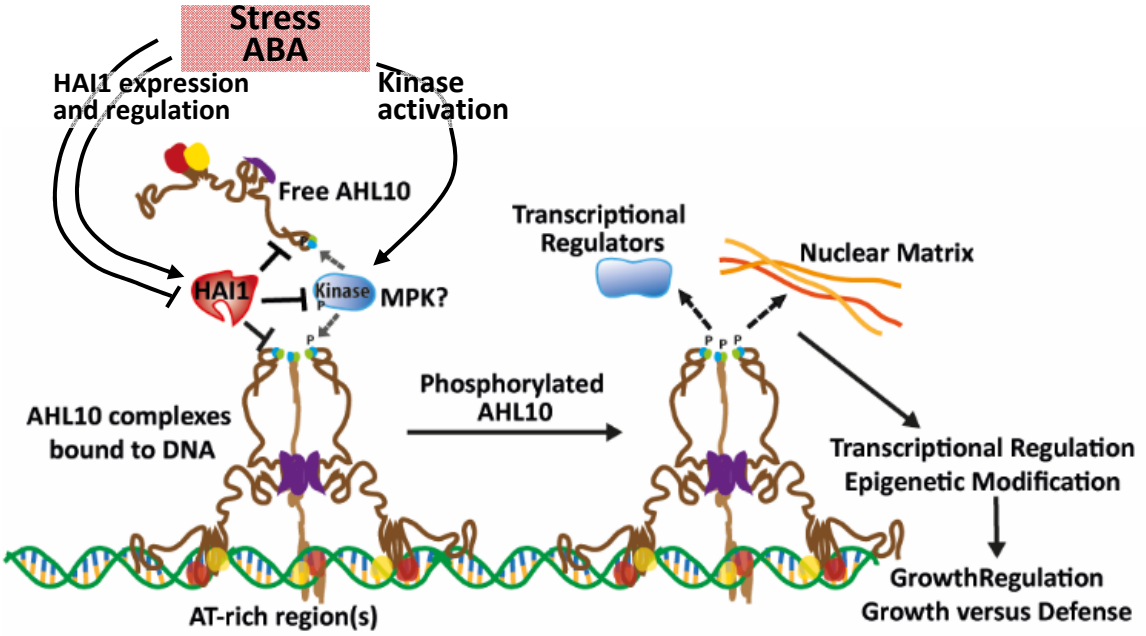

SI Appendix Figure S14: Model of AHL10 function and its regulation by HAI1.
Previous analysis of AHLs indicates that they may bind DNA as trimers with each AHL in the complex binding either to adjacent DNA sites or to more distal sites to bring them together in the same regulatory complex. HAI1 dephosphorylates AHL10. This likely occurs on free AHL10 in the nucleoplasm (as the BiFC interactions of HAI1 and AHL10 do not show nuclear foci) but could also occur within DNA bound AHL complexes. HAI1 dephosphorylation is counteracted by phosphorylation by unknown kinase(s). HAI1 may also regulate AHL10 phosphorylation by dephosphorylating these kinase(s) which phosphorylate AHL10. The presence of an SP motif at the AHL10 S314 phosphorylation site, as well as previous finding that AHL13 is a putative MPK substrate, suggests phosphorylation by MPK(s). This is also consistent with known MPK functions in stress signaling and demonstration that HAI1 can dephosphorylate MPK3 and MPK6. Both HAI1 and kinase activity are regulated by environmental and hormone signals to influence AHL10 phosphorylation. AHL10 S314 phosphorylation does not affect the formation of AHL10 complexes (as indicated by rBiFC analysis) but does affect the localization of AHL10 complexes in nuclear foci. These foci may represent sites of nuclear matrix attachment as proposed for other AHLs; however, further investigation will be needed to establish the nature of AHL10 foci. The variable C-terminal region where the AHL10 S314 phosphorylation site is located has been proposed to be involved in AHL interaction with diverse types of transcriptional regulators. Thus, S314 phosphorylation may also affect AHL10 interaction with other transcriptional regulators. In either case, S314 phosphorylation is required for AHL10 function in transcriptional regulation, perhaps related to epigenetic mechanisms as previously found for AHL10. This leads to altered expression of a set of genes involved in AHL10-dependent growth regulation at low water potential and which may be more broadly involved in growth versus defense coordination.